

Forward sliding-swing acceleration: electron acceleration by high-intensity lasers in strong plasma magnetic fields

Z. Gong^{1,2}, F. Mackenroth^{3,4}, T. Wang⁴, X. Q. Yan¹, T. Toncian⁵, and A. V. Arefiev⁴

¹*Peking University, Beijing 100871, China*

²*Center for High Energy Density Science, The University of Texas at Austin, Austin, TX 78712, USA*

³*Max Planck Institute for the Physics of Complex Systems, 01187 Dresden, Germany*

⁴*University of California at San Diego, La Jolla, CA 92093, USA and*

⁵*Institute for Radiation Physics, Helmholtz-Zentrum Dresden-Rossendorf e.V., 01328 Dresden, Germany*

(Dated: December 15, 2024)

A high-intensity laser beam propagating through a dense plasma drives a strong current that robustly sustains a strong quasi-static Mega Tesla-level azimuthal magnetic field. The transverse laser field efficiently accelerates electrons in the presence of such a field that confines the transverse motion and deflects the electrons in the forward direction, establishing the novel *forward-sliding swing acceleration* mechanism. Its advantage is a threshold rather than resonant behavior, accelerating electrons to high energies for sufficiently strong laser-driven currents. We study the electrons' dynamics by a simplified model analytically, specifically deriving simple relations between the current, the particles' initial transverse momenta and the laser's field strength classifying the energy gain. We confirm the model's predictions by numerical simulations, indicating Mega ampere-level threshold currents and energy gains two orders of magnitude higher than achievable without the magnetic field.

Recent advancements in high-power laser technology [1, 2] have paved the way for multidisciplinary applications by enabling compact plasma-based sources of energetic particles, such as electrons [3], ions [4–6], positrons [7, 8], and neutrons [9], and radiation [10, 11], ranging from x-rays to hard gamma-rays. For these applications the energy transfer from the laser pulse to the plasma electrons is critically important, as once accelerated, they can drive secondary particle and radiation sources. The applications that prioritize the mono-energetic feature of the electron spectrum tend to rely on the laser-wakefield acceleration regime [3, 12], whereas the applications that prioritize the electron charge tend to rely on the direct laser acceleration (DLA) regime [13, 14]. The latter include bright, short-pulsed gamma-ray sources [15–20] that are necessary for advanced nuclear and radiological detection systems [21, 22].

The essence of DLA is an energy transfer from the laser electric field directly to the electrons. This can take place in a dense plasma without stringent density limitations [23, 24], which allows the laser to accelerate a large electron population. The regime can even be used to accelerate electrons in optically opaque plasmas if the laser is sufficiently intense to induce relativistic transparency [25, 26]. Typically, the accelerated electrons are pulled into the laser beam from the surrounding plasma with an initially transverse momentum. An electron with initial momentum $p_i \gg m_e c$ can gain an energy $\varepsilon_0 = \gamma_0 m_e c^2$, where $\gamma_0 \approx (a_0^2/2)(m_e c/p_i)$, from a plane wave with intensity I_0 and normalized amplitude $a_0 \approx 0.85 I_0 [10^{18} \text{ W/cm}^2]^{1/2} \lambda [\mu\text{m}]$ where λ is the wavelength, m_e the electron mass (charge $e < 0$), and c the speed of light. The suppression $\gamma_0 \propto 1/p_i$ is due to the electron dephasing from the laser pulse [27].

A lot of research has been dedicated to mitigating the

negative impact of the dephasing in order to increase the electron energy gain [13, 28, 29]. Quasi-static electric fields caused by charge separation have been shown to alter the dephasing, which leads to an enhanced energy exchange between the electrons and the laser [30]. However, this principle is not applicable at next generation laser facilities, such as ELI [31], Apollon [32], and XCELS [33], whose pulses would induce such strong transverse plasma electric fields that the ion motion would become important on time scales shorter than the pulse duration. The resulting transverse ion motion has been shown to dramatically reduce the quasi-static electric fields needed for achieving the electron energy enhancement [34].

High-intensity lasers additionally drive longitudinal electron currents through the plasma, causing strong quasi-static azimuthal magnetic fields. In contrast to the electric fields, these fields are robust with respect to the ion motion and can be sustained at ultra high intensities [17, 34]. Furthermore, in such magnetic fields an electron's motion exhibits a forward drift at constant velocity and dominantly transverse oscillations in a reference frame moving with this drift velocity. This motion can be visualized as a forward sliding swing. In the presence of an additional laser field, the forward sliding motion leads to dephasing such that the laser can directly accelerate the electron along their instantaneous velocity, implying energy gain (s. Fig. 1). Hence, we label the mechanism *forward-sliding swing acceleration* (FSSA).

In this Letter, we show that in the FSSA regime a strong azimuthal magnetic field dramatically enhances the electron energy gain from a laser field in a threshold process. We analytically examine the electron dynamics to find a critical current needed to sustain a sufficiently strong magnetic field that leads to an enhanced energy gain regardless of the transverse electron momentum.

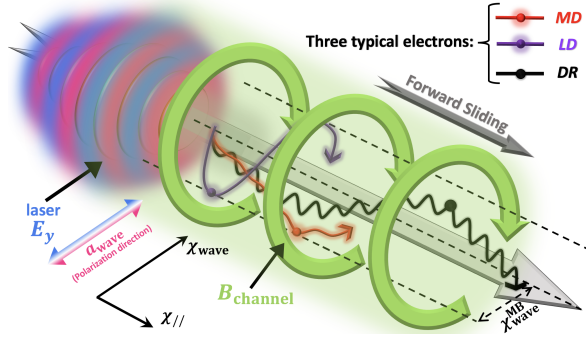


FIG. 1: Schematic diagram of FSSA, where the laser propagation along χ_{\parallel} defines the forward sliding direction. Three different regimes are exemplified: Red, grape and black lines depict momentum dominated (MD), laser dominated (LD) and deflection regime (DR), respectively. The laser polarization is along the direction of χ_{wave} .

The advantage of this regime is that it can be employed to generate large numbers of highly energetic electrons by irradiating a solid-density material with an ultra-high intensity laser. Such dense high-energy bunches may be the key to driving the bright gamma-ray sources mentioned above.

To illustrate the FSSA mechanism clearly, we note that the net electron motion is longitudinal through a longitudinally static ion background, largely compensating the electrons' space charge. Additionally, we assume the plasma to turn relativistically transparent enabling the intense laser pulse to propagate inside it. We can then capture the characteristic features of the electron dynamics in a single particle model inside a prescribed combination of the laser and quasi-static magnetic fields (s. Fig. 1). This field configuration was also observed in fully self-consistent kinetic plasma simulations, where the magnetic field generated by a homogeneous current J_0 in a cylindrical channel with radius r was found to be well characterized by $\alpha = (\lambda/r)^2 J_0 / (4\pi J_A)$ where $J_A = m_e c^3 / |e| \approx 17$ kA is the Alfvén current [17].

We consequently study an electron in a monochromatic, linearly polarized plane laser wave propagating in x_{\parallel} -direction and polarized along \mathbf{e}_{wave} with electric and magnetic fields given by $\mathbf{E}_{\text{wave}} = -m_e c / |e| \partial \mathbf{a}_{\text{wave}} / \partial t$ and $\mathbf{B}_{\text{wave}} = m_e c^2 / |e| \nabla \times \mathbf{a}_{\text{wave}}$ for a vector potential $\mathbf{a}_{\text{wave}}(t, \mathbf{x}) = a_0 \cos(\xi + \xi_0) \mathbf{e}_{\text{wave}}$, where $\xi = \tau - \chi_{\parallel}$ with the dimensionless parameters $\tau = \omega_0 t$, $\chi = \omega_0 \mathbf{x} / c$, $\boldsymbol{\pi} = \mathbf{p} / mc$, $\gamma = \varepsilon / mc^2$, where $\omega_0 = (2\pi c) / \lambda$ is the laser frequency, $\varepsilon(\mathbf{p})$ the electron's instantaneous energy (momentum), and ξ_0 the initial phase. The azimuthal magnetic field is given by $\mathbf{B}_{\text{mag}} = m_e c^2 / |e| \nabla \times \mathbf{a}_{\text{mag}} \propto \mathbf{e}_{\theta}$, derived from $\mathbf{a}_{\text{mag}} = \alpha(\chi_{\text{wave}}^2 + \chi_{\perp}^2) \mathbf{e}_{\parallel}$ with the reduced coordinate χ_{\perp} perpendicular to the laser's propagation and polarization directions.

The particle dynamics are governed by the relativistic Lorentz equation, which gives the constant of motion

$\gamma - \pi_{\parallel} + \alpha \chi_{\text{wave}}^2 = C_1$, provided radiation reaction [35–39] and QED effects [40–42], important at higher energies [43–45], are negligible. We are going to consider a relativistic electron moving initially in transverse direction $\boldsymbol{\pi}(\xi = 0) = \pi_i \mathbf{e}_{\text{wave}}$ on axis $\chi_{\text{wave}}(\xi = 0) = 0$, mimicking the electron injection previously observed in kinetic plasma simulations [17]. For $\pi_i \gg 1$ it is $C_1 = \gamma \approx \pi_i$. Furthermore, we see that without the magnetic field the dephasing $R := \gamma(d\xi/dt) = \gamma - \pi_{\parallel} = \text{const.}$ With the azimuthal magnetic field, however, the dephasing depends on the electron's transverse position according to

$$R = \pi_i - \alpha \chi_{\text{wave}}^2(\tau, \boldsymbol{\chi}). \quad (1)$$

The transverse momentum π_{wave} is determined by

$$\frac{d}{d\xi} (\pi_{\text{wave}} - a_{\text{wave}}) = -\frac{\pi_{\parallel}}{R} \frac{\partial a_{\text{mag}}}{\partial \chi_{\text{wave}}}. \quad (2)$$

Substituting $\pi_{\parallel}(\chi_{\text{wave}}, d\chi_{\text{wave}}/d\xi)$ and $R(\chi_{\text{wave}})$ into Eq. (2) it can be reduced to the second order nonlinear differential equation

$$\chi_{\text{wave}}'' - \frac{\alpha \chi_{\text{wave}} \chi_{\text{wave}}'^2}{R} + \frac{\alpha \chi_{\text{wave}}}{R^3} - \frac{\alpha \chi_{\text{wave}}}{R} = \frac{a'_{\text{wave}}}{R}, \quad (3)$$

where the prime denotes $d/d\xi$.

Before we turn to a quantitative numerical solution of this equation, we provide a qualitative analysis in limiting cases. First we note that the electron's energy $\gamma(\xi)$ evolves according to

$$\frac{d\gamma}{d\xi} = -\left(\frac{\pi_{\text{wave}}}{R}\right) a_0 \sin(\xi + \xi_0). \quad (4)$$

From this expression we infer that the electron gains energy only from the laser field, as it must be, and that the laser's periodic oscillations will cancel any energy gain, unless $R \rightarrow 0$ over a phase interval $\xi < 2\pi$. On the other hand, from Eq. (1) we conclude that $R \rightarrow 0$ only if $\chi_{\text{wave}} \rightarrow \chi_{\text{wave}}^{\text{MB}} := \sqrt{\pi_i / \alpha}$. Interestingly, in the geometry introduced above already the azimuthal magnetic field alone will confine the electron motion to transverse excursions $\chi_{\text{wave}} \leq \chi_{\text{wave}}^{\text{MB}}$, whence we label this value the *magnetic boundary* (MB). Since the electron's motion is in $(\chi_{\parallel}, \chi_{\text{wave}})$ -plane, the maximum magnetic field, which the electron can experience, is $B_{\text{max}} = 2\sqrt{\pi_i} \alpha$ when $\chi_{\text{wave}} \rightarrow \chi_{\text{wave}}^{\text{MB}}$. Now we study two particular cases in which $\chi_{\text{wave}} \rightarrow \chi_{\text{wave}}^{\text{MB}}$ is possible: the *momentum dominated* (MD) regime ($\pi_i \gg a_0 \gg 1$) and the *laser dominated* (LD) regime ($1 < \pi_i \ll a_0$).

Momentum dominated regime — The laser-induced transverse momentum can be regarded as a small perturbation of the electron's large initial momentum. As discussed above, the magnetic field alone would reflect the electron at the MB and a comparatively weak laser will not disturb this behavior strongly. We can derive a quantitative threshold above which transverse momenta

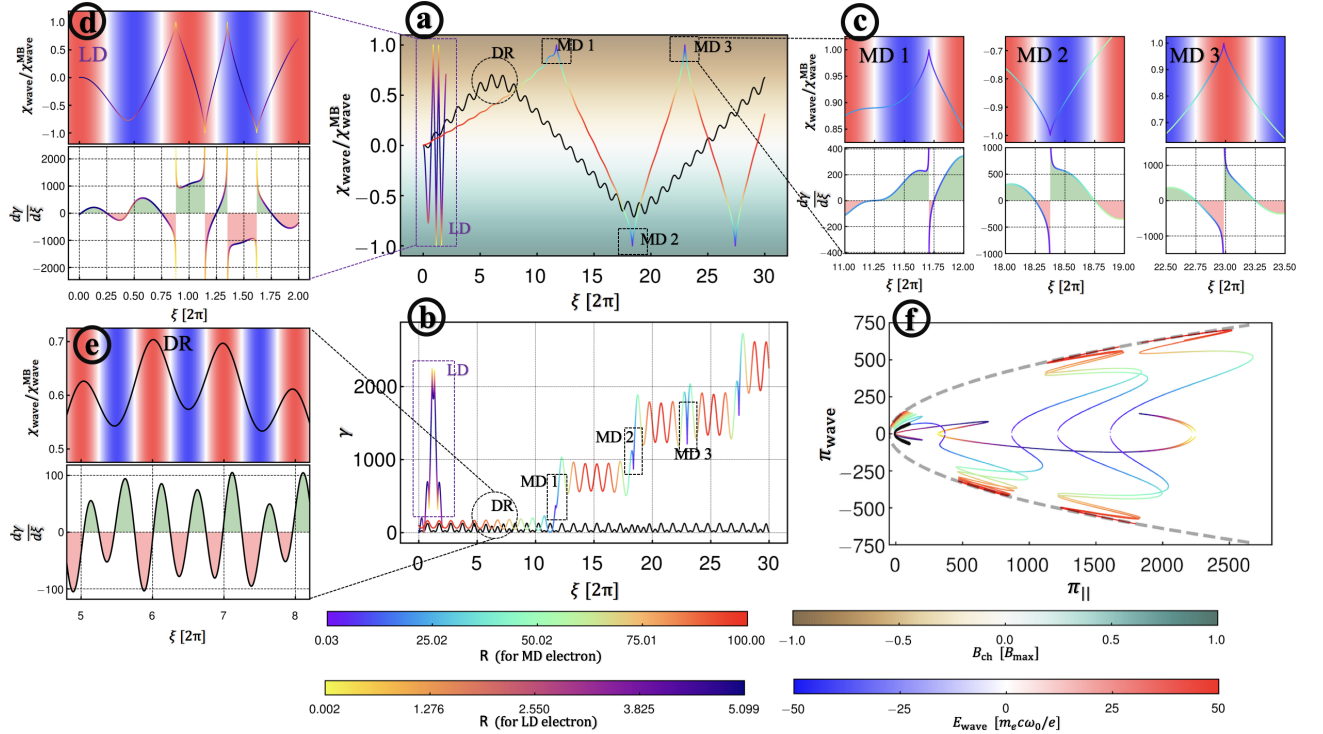


FIG. 2: (a) Numerically obtained trajectories in three different regimes: MD ($\pi_i = 100$), LD ($\pi_i = 5$) and DR ($\pi_i = 25$) with R in rainbow, magma and black color, respectively. (b) Electron energy (same color code as (a)). (c) Zoom in on MD regime turning points in position (upper panel) and energy space (lower panel) indicating the asymmetry of $d\gamma/d\xi$. (d) and (e) are the same as (c) but for the LD and DR case, respectively. (f) Electron evolution in $(\pi_{\parallel}, \pi_{\text{wave}})$ -space, where the dashed gray line indicates the limiting trajectory $\pi_{\parallel} = (1 + \pi_{\text{wave}}^2 - R^2)/(2R)$ for $R = 100.0$.

the MD region is accessed by comparing the time scales on which the magnetic and laser fields act on the electron, respectively. Obviously the magnetic field will deflect the electron's initial transverse momentum fully into longitudinal motion $\pi^{\parallel} \sim \pi^0$ on a time scale $\tau^{\text{mag}} \sim \chi_{\text{wave}}^{\text{MB}}$. On the other hand, averaging the momentum of an electron inside a plane wave [46] over one laser period, it can be estimated that each period the laser field imparts a longitudinal momentum of order $\langle \pi_{\text{las}}^{\parallel} \rangle \lesssim a_0^2/\pi_i$ onto the electron. Hence, in order to impart a longitudinal momentum $\pi^{\parallel} \sim \pi_i$ onto the electron the laser needs a time $\tau^{\text{laser}} \gtrsim \pi_i^2/a_0^2$. In the MD regime, the laser field must not act on time scales shorter than the magnetic field, or else it would yield the main effect on the electron motion. Consequently, we expect the MD regime to be accessible in the regime $\tau^{\text{mag}} \leq \rho\tau^{\text{laser}}$, where ρ is a free parameter accounting for enhancements of the laser acceleration over the case without magnetic field. Expressed in terms of the initial transverse momentum this condition reads

$$\pi_i \geq \pi_{\text{MD}} := a_0^{\frac{4}{3}} \alpha^{-\frac{1}{3}} \rho^{-\frac{2}{3}}. \quad (5)$$

Laser dominated regime — The initial momentum is small enough for the electron's transverse momentum to be dominated by the laser field. We note that in this regime $\chi_{\text{wave}}^{\text{MB}}$ can become small, whereas the

plane laser wave transversely displaces the electron by $\chi_{\text{p.w.}}^{\text{max}} \sim 1 + a_0/\pi_i$ within one period [46, 47]. As soon as $\chi_{\text{p.w.}}^{\text{max}} > \chi_{\text{wave}}^{\text{MB}}$ the dominating laser dynamics will drive the electron close to the MB, whence it can again acquire net energy. Neglecting the unity in $\chi_{\text{p.w.}}^{\text{max}}$, originating from the electron's initial momentum, we can recast the above condition for the onset of the LD regime to read $a_0/\pi_i \geq \kappa\sqrt{\pi_i/\alpha}$ where $\kappa \in [0, 1]$ is a free parameter accounting for deviations from the laser-driven plane wave dynamics inside the weak azimuthal magnetic field. Solving the above condition for π_i we find the LD regime to be accessible for initial electron momenta satisfying

$$\pi_i \leq \pi_{\text{LD}} = \alpha^{\frac{1}{3}} a_0^{\frac{2}{3}} \kappa^{-\frac{2}{3}}. \quad (6)$$

It follows from Eqs. (5) and (6) that there can be a third regime with $\pi_{\text{LD}} < \pi_i < \pi_{\text{MD}}$. In this regime, we expect the laser field to be too weak to drive the electron close to $\chi_{\text{wave}}^{\text{MB}}$ but at the same time strong enough for π_{wave} to frequently change its sign. Hence, FSSA will not be effective here. We label this regime the *deflection regime* (DR). It disappears with the increase of α at $\pi_{\text{MD}} = \pi_{\text{LD}}$, which occurs at $\alpha = \alpha^* \equiv a_0\kappa/\rho$. An important conclusion is that the energy enhancement takes place regardless of the initial electron momentum beyond this threshold for $\alpha \geq \alpha^*$.

To now test these analytical estimates and fix the free parameters in Eqs. (5,6) we integrate Eq. (3) numerically. We study a laser of amplitude $a_0 = 50$ and wavelength $\lambda = 1 \mu\text{m}$, a normalized electron current density $\alpha = 0.01$ and an electron injected into the plasma at the initial phase $\xi_0 = \pi/2$. We begin by studying the MD regime, to which end we choose $\pi_i = 100 \gtrsim a_0$. In this regime, the laser field does not induce a sign flip of π_{wave} and the electron will continuously approach the MB. We then study an exemplary electron trajectory (s. Fig. 2(a) and Fig. 2(b)), along which the rainbow color bar gives the dephasing R . We see that indeed the electron accumulates energy exclusively around the trajectory's turning points where $\chi_{\text{wave}} \rightarrow \chi_{\text{wave}}^{\text{MB}}$ ($R \rightarrow 0$). In particular, at three turning points we study the electron's transverse position, relative to the laser field and energy gain $d\gamma/d\xi$ (s. Fig. 2(c)). While at MD1 and MD2 $d\gamma/d\xi$ is anti-symmetric in phase and the electron effectively absorbs energy from the laser field, at the turning point MD3 the net energy gain is small since it coincidentally occurs in phase with the laser field. In momentum space the electron's oscillatory behavior with discrete jumps to higher energy levels is clearly visible (s. Fig. 2(f)).

Next, we study the LD regime by choosing $\pi_i = 5 \ll \pi_{\text{LD}} = 13.47 \ll a_0$. In contrast to the MD regime the electron approaches the MB at every laser period (s. Fig. 2(d)). As a result, the electron accumulates more energy than achievable without the magnetic field $\gamma \approx 2000 \approx 4\gamma_0$ (s. Fig. 2(b)). In momentum space we find the electron trajectory in the LD regime, in contrast to the MD regime, to jump to high energies within a single laser cycle (s. Fig. 2(f)).

To visualize the intermediate, non-accelerating DR regime we choose $\pi_{\text{LD}} < \pi_i = 25 < \pi_{\text{MD}}$. In this regime the electron does not approach the MB (black line in Fig. 2(a)) and its minimum dephasing at the maximum transverse position is $R_{\text{min}} \approx 14$. Consequently, the absorbed energy is always oscillating (s. Fig. 2(e)) and the net energy gain is small (s. Fig. 2(b)).

To highlight the broad parameter range in which FSSA is feasible, we present a detailed numerical parameter scan of the electron's maximal energy gain γ_{max} normalized to the energy gain without magnetic field γ_0 as a function of the initial momentum π_i and the normalized current α (s. Fig. 3(a)). Fitting the free parameters of the above derived scalings (5, 6) we find $\rho \approx 125$ and $\kappa \approx 0.14$, yielding good agreement between the numerical data and the analytical curves. Furthermore, with these parameters we find the current beyond which an electron is accelerated independently of p_i to be

$$J_0^* = \frac{(4\pi)\alpha^* r^2}{\lambda^2} J_A \approx 0.24 a_0 \left(\frac{r}{\lambda}\right)^2 \text{ kA}. \quad (7)$$

Two conditions must be satisfied for the discussed model to be applicable. The first condition is that the

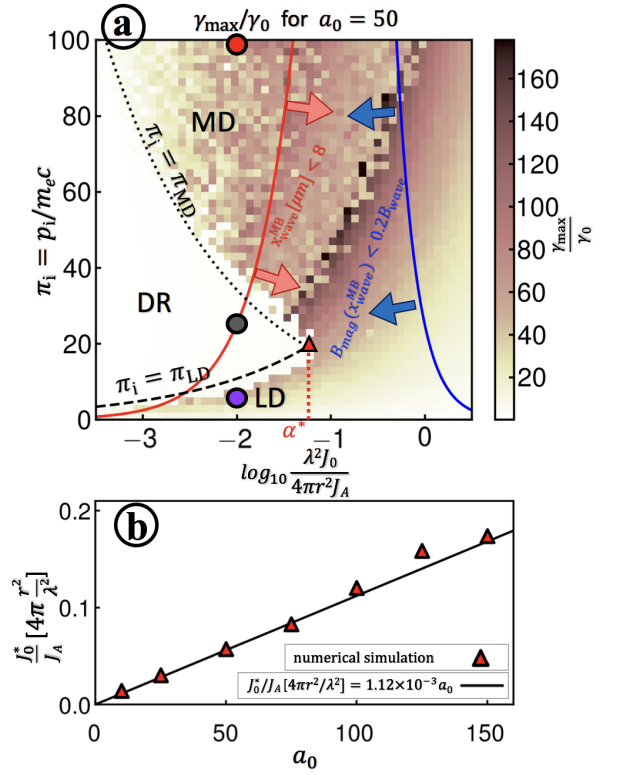


FIG. 3: (a) Numerical parameter scan of $\gamma_{\text{max}}/\gamma_0$ for $a_0 = 50$, where $\gamma_0 = a_0^2/2\pi_i$. The red (MD), black (DR) and purple (LD) circles correspond to the three case in Fig. 2. The black dotted (dashed) line gives the threshold from Eq. (5) (Eq. (6)). The right (left) side of the solid red (blue) line denotes the region for which $x_{\text{wave}}^{\text{MB}} < 8\mu\text{m}$ ($B_{\text{mag}}(x_{\text{wave}}^{\text{MB}}) < 0.2B_{\text{wave}}$). The red triangle indicates the threshold α^* . (b) Comparison of numerical results (red triangles) to the analytical scaling of Eq. (7) (solid black line).

width of the laser beam w_0 must exceed the size of the region inside the magnetic boundary, i.e. $w_0 > x_{\text{wave}}^{\text{MB}}$. The second condition is that the plasma magnetic field inside the region set by the magnetic boundary must be significantly below the magnetic field of the laser, i.e. $B_{\text{mag}}(x_{\text{wave}}^{\text{MB}}) \ll B_{\text{wave}}$, for the laser to be able to drive this field. These conditions are not mutually exclusive, as illustrated in Fig. 3 for $w_0 = 8\mu\text{m}$ and $B_{\text{mag}}(x_{\text{wave}}^{\text{MB}}) < 0.2B_{\text{wave}}$. The corresponding laser power of 7 PW should be available at state-of-the-art laser facilities. According to Eq. (7), the plasma current must exceed $J_0^* \approx 0.8 \text{ MA} \gg J_A$. Lastly, we assumed the laser's phase velocity to be c , which is reasonable for a highly relativistically transparent plasma. The FSSA mechanism consequently requires a plasma of density $n \ll a_0 n_{\text{cr}}$, where we assumed the plasma to be cold and $n_{\text{cr}} = m_e \pi c^2 / \lambda^2 e^2 \approx 1.1 \times 10^{21} \text{ cm}^{-3} (\lambda[\mu\text{m}])^{-2}$ is the nonrelativistic critical density. Consequently, in the above studied example FSSA operates efficiently provided $n \lesssim 50 n_{\text{cr}} \approx 5 \times 10^{22} \text{ cm}^{-3}$, close to solid densities.

In conclusion, in this manuscript we identified and

characterized the novel, direct *forward-sliding swing acceleration* (FSSA) mechanism, steered by an intense laser propagating through a dense plasma generating an azimuthal magnetic field. In this field combination an electron accumulates kinetic energy exclusively close to the magnetic boundaries, beyond which the azimuthal magnetic field inhibits electron motion. We identified two regimes in which the electron can approach this boundary and demonstrated that for currents exceeding the threshold J_0^* it is accelerated to high energies regardless of its initial momentum. This clarifies how electrons absorb energy from the studied, complex field structure and indicates that the FSSA mechanism can facilitate gamma-ray emission [17–20].

The work has been supported by the National Science Foundation (Grant No. 1632777), the National Basic Research Program of China (Grant No.2013CBA01502), and NSFC (Grant No. 11535001).

-
- [1] D. Strickland and G. Mourou, Optics communications **55**, 447 (1985).
- [2] G. A. Mourou, T. Tajima, and S. V. Bulanov, Rev. Mod. Phys. **78**, 309 (2006).
- [3] E. Esarey, C. Schroeder, and W. Leemans, Reviews of Modern Physics **81**, 1229 (2009).
- [4] H. Daido, M. Nishiuchi, and A. S. Pirozhkov, Reports on Progress in Physics **75**, 056401 (2012).
- [5] A. Macchi, M. Borghesi, and M. Passoni, Reviews of Modern Physics **85**, 751 (2013).
- [6] F. Mackenroth, A. Gonoskov, and M. Marklund, Phys. Rev. Lett. **117**, 104801 (2016).
- [7] H. Chen, S. C. Wilks, J. D. Bonlie, E. P. Liang, J. Myatt, D. F. Price, D. D. Meyerhofer, and P. Beiersdorfer, Physical review letters **102**, 105001 (2009).
- [8] H. Chen, S. Wilks, D. Meyerhofer, J. Bonlie, C. Chen, S. Chen, C. Courtois, L. Elberson, G. Gregori, W. Kruer, et al., Physical review letters **105**, 015003 (2010).
- [9] I. Pomerantz, E. Mccary, A. R. Meadows, A. Arefiev, A. C. Bernstein, C. Chester, J. Cortez, M. E. Donovan, G. Dyer, E. W. Gaul, et al., Physical review letters **113**, 184801 (2014).
- [10] S. Corde, K. T. Phuoc, G. Lambert, R. Fitour, V. Malka, A. Rousse, A. Beck, and E. Lefebvre, Reviews of Modern Physics **85**, 1 (2013).
- [11] F. Albert and A. G. R. Thomas, Plasma Physics and Controlled Fusion **58**, 103001 (2016).
- [12] T. Tajima and J. Dawson, Physical Review Letters **43**, 267 (1979).
- [13] A. Pukhov, Z.-M. Sheng, and J. Meyer-ter Vehn, Physics of Plasmas **6**, 2847 (1999).
- [14] A. V. Arefiev, B. N. Breizman, M. Schollmeier, and V. N. Khudik, Physical review letters **108**, 145004 (2012).
- [15] L. Ji, A. Pukhov, I. Y. Kostyukov, B. Shen, and K. Akli, Physical review letters **112**, 145003 (2014).
- [16] L. Ji, A. Pukhov, E. Nerush, I. Y. Kostyukov, B. Shen, and K. Akli, Physics of Plasmas **21**, 023109 (2014).
- [17] D. Stark, T. Toncian, and A. Arefiev, Physical review letters **116**, 185003 (2016).
- [18] T. Huang, A. Robinson, C. Zhou, B. Qiao, B. Liu, S. Ruan, X. He, and P. Norreys, Physical Review E **93**, 063203 (2016).
- [19] A. Gonoskov, A. Bashinov, S. Bastrakov, E. Efimenko, A. Ilderton, A. Kim, M. Marklund, I. Meyerov, A. Muraviev, and A. Sergeev, Physical Review X **7**, 041003 (2017).
- [20] Z. Gong, R. H. Hu, H. Y. Lu, J. Q. Yu, D. H. Wang, E. G. Fu, C. E. Chen, X. T. He, and X. Q. Yan, Plasma Physics and Controlled Fusion **60**, 044004 (2018).
- [21] E. C. Schreiber, R. Canon, B. Crowley, C. Howell, J. Kelley, V. Litvinenko, S. Nelson, S. Park, I. Pinayev, R. Prior, et al., Physical Review C **61**, 061604 (2000).
- [22] E. Kwan, G. Rusev, A. Adekola, F. Döna, S. Hammond, C. Howell, H. Karwowski, J. Kelley, R. S. Pedroni, R. Raut, et al., Physical Review C **83**, 041601 (2011).
- [23] B. Liu, H. Wang, J. Liu, L. Fu, Y. Xu, X. Yan, and X. He, Physical review letters **110**, 045002 (2013).
- [24] L. Willingale, A. V. Arefiev, G. J. Williams, H. Chen, F. Dollar, A. U. Hazi, A. Maksimchuk, M. J.-E. Manuel, E. Marley, W. Nazarov, et al., New Journal of Physics **20**, 093024 (2018).
- [25] S. Palaniyappan, B. M. Hegelich, H.-C. Wu, D. Jung, D. C. Gautier, L. Yin, B. J. Albright, R. P. Johnson, T. Shimada, S. Letzring, et al., Nature Physics **8**, 763 (2012).
- [26] D. J. Stark, C. Bhattacharjee, A. V. Arefiev, T. Toncian, R. Hazeltine, and S. Mahajan, Physical review letters **115**, 025002 (2015).
- [27] A. Arefiev, V. Khudik, A. Robinson, G. Shvets, L. Willingale, and M. Schollmeier, Physics of Plasmas **23**, 056704 (2016).
- [28] A. Robinson, A. Arefiev, and D. Neely, Physical review letters **111**, 065002 (2013).
- [29] A. Arefiev, A. Robinson, and V. Khudik, Journal of Plasma Physics **81** (2015).
- [30] V. Khudik, A. Arefiev, X. Zhang, and G. Shvets, Physics of Plasmas **23**, 103108 (2016).
- [31] Extreme light infrastructure project, www.eli-laser.eu.
- [32] J. Zou, C. Le Blanc, D. Papadopoulos, G. Chériaux, P. Georges, G. Mennerat, F. Druon, L. Lecherbourg, A. Pellegrina, and P. Ramirez, High Power Laser Science and Engineering **3**, e2 (2015).
- [33] Exawatt center for extreme light studies, www.xcels.iapras.ru.
- [34] O. Jansen, T. Wang, D. Stark, E. d’Humières, T. Toncian, and A. Arefiev, Plasma Physics and Controlled Fusion (2018).
- [35] L. D. Landau and E. M. Lifshitz (1971).
- [36] A. Thomas, C. Ridgers, S. Bulanov, B. Griffin, and S. Mangles, Physical Review X **2**, 041004 (2012).
- [37] A. Gonoskov, A. Bashinov, I. Gonoskov, C. Harvey, A. Ilderton, A. Kim, M. Marklund, G. Mourou, and A. Sergeev, Physical review letters **113**, 014801 (2014).
- [38] J. M. Cole, K. T. Behm, E. Gerstmayr, T. G. Blackburn, J. C. Wood, C. D. Baird, M. J. Duff, C. Harvey, A. Ilderton, A. S. Joglekar, et al., Phys. Rev. X **8**, 011020 (2018).
- [39] K. Poder, M. Tamburini, G. Sarri, A. Di Piazza, S. Kuschel, C. D. Baird, K. Behm, S. Bohlen, J. M. Cole, D. J. Corvan, et al., Phys. Rev. X **8**, 031004 (2018).
- [40] F. Mackenroth and A. Di Piazza, Phys. Rev. A **83**, 032106 (2011).

- [41] A. Di Piazza, C. Müller, K. Hatsagortsyan, and C. Keitel, *Reviews of Modern Physics* **84**, 1177 (2012).
- [42] F. Mackenroth and A. Di Piazza, *Phys. Rev. Lett.* **110**, 070402 (2013).
- [43] S. Bulanov, T. Z. Esirkepov, Y. Hayashi, M. Kando, H. Kiriyama, J. Koga, K. Kondo, H. Kotaki, A. Pirozhkov, S. Bulanov, et al., *Nuclear Instruments and Methods in Physics Research Section A: Accelerators, Spectrometers, Detectors and Associated Equipment* **660**, 31 (2011).
- [44] F. Mackenroth, N. Neitz, and A. Di Piazza, *Plasma Physics and Controlled Fusion* **55**, 124018 (2013).
- [45] S. Bulanov, T. Z. Esirkepov, M. Kando, J. Koga, K. Kondo, and G. Korn, *Plasma Physics Reports* **41**, 1 (2015).
- [46] J. W. Meyer, *Phys. Rev. D* **3**, 621 (1971).
- [47] A. V. Arefiev, V. N. Khudik, and M. Schollmeier, *Physics of Plasmas* **21**, 033104 (2014).